



1 **Contributions of different anthropogenic volatile organic compound**
2 **sources to ozone formation at a receptor site in the Pearl River Delta**
3 **region and its policy implications**

4 Zhuoran He^{1,2}, Xuemei Wang³, Zhenhao Ling^{1,2*}, Jun Zhao^{1,2}, Hai Guo⁴, Min Shao³, Zhe Wang^{4,*}

5 ¹School of Atmospheric Sciences, Sun Yat-sen University, Guangzhou, China

6 ²Guangdong Province Key Laboratory for Climate Change and Natural Disaster Studies, Sun Yat-sen University, Guangzhou,
7 China

8 ³Institute for Environmental and Climate Research, Jinan University, Guangzhou, China

9 ⁴Department of Civil and Environmental Engineering, Hong Kong Polytechnic University, Hong Kong, China

10 *Correspondence to:* lingzh3@mail.sysu.edu.cn (Zhenhao Ling); z.wang@polyu.edu.hk (Zhe Wang)

11 **Abstract.** Volatile organic compounds (VOCs) are key precursors of photochemical smog. Quantitatively
12 evaluating the contributions of VOCs sources to ozone (O₃) formation could provide valuable information
13 for emissions control and photochemical pollution abatement. This study analysed the continuously
14 measured VOCs during the photochemical season in 2014 at a receptor site (Heshan site, HS) in the Pearl
15 River Delta (PRD) region, where photochemical pollution has been a long-standing issue. The averaged
16 mixing ratio of measure VOCs was 34 ± 3 ppbv, with the largest contribution from alkanes (17 ± 2 ppbv,
17 49%), followed by aromatics, alkenes, and acetylene. The positive matrix factorization (PMF) model was
18 applied to resolve the anthropogenic sources of VOCs, coupled with a photochemical-aged-based
19 parameterization that better considers the photochemical processing effects. Four anthropogenic emission
20 sources were identified and quantified, with gasoline vehicular emission as the most significant
21 contributor to the observed VOCs, followed by diesel vehicular emissions, biomass burning, and solvent
22 usage. The O₃ photochemical formation regime at HS was identified as VOCs-limited by a photochemical
23 box model with the master chemical mechanism (PBM-MCM). The PBM-MCM model results also
24 suggested that vehicular emission was the most important source to the O₃ formation, followed by
25 biomass burning and solvent usage. Sensitivity analysis indicated that in order to prevent the increment



26 of O₃ concentration, the abatement ratios of the individual VOC source vs. NO_x should be higher than
27 3.8, 4.6, 4.6, and 3.3, respectively, for diesel vehicular emission, solvent usage, biomass burning, and
28 gasoline vehicular emission, respectively. Based on the above results, a brief review on the policies on
29 the controlling of vehicular emissions and biomass burning in the PRD region from a regional perspective
30 were also provided in this study. It reveals that different policies have been/being implemented and
31 formulated could help to alleviate the photochemical pollution in the PRD. Nevertheless, evaluation on
32 the cost-benefit of each policy is still needed to improve the air quality.

33 Key words: Anthropogenic emissions; Ozone formation; Pearl River Delta region; Policy implications

34 1 Introduction

35 Atmospheric volatile organic compounds (VOCs) have significant impact on air quality. Due to their high
36 chemical activity, VOCs are key precursors of ozone (O₃) and secondary organic aerosol (SOA). In
37 addition, some VOCs and their oxidation products are harmful to human health, which further deteriorates
38 air quality (Seinfeld and Pandis, 2006; ATSDR, 2007; Huang et al., 2014). VOCs have a variety of natural
39 and anthropogenic sources, including biogenic emissions and emissions from human activities (*i.e.*, fuel
40 and biomass combustion, fuel evaporation, solvent usage, industrial processes, etc.). It is relatively well
41 known that the two key ozone precursors (VOCs and NO_x) synergize complex, nonlinear effects on ozone
42 formation. For a given region, depending on which precursor is the limiting factor for controlling ozone
43 formation, the ozone isopleth diagram (the mixing ratios of VOCs and NO_x as two coordinates) can be
44 classified into VOCs and NO_x limited regimes. In the VOCs-limited regime, the effective measure for
45 reducing ozone production is to control the VOC emissions and vice versa for the NO_x-limited regime
46 (Jenkin and Clemitshaw, 2000).

47 In recent years, with rapid urbanization and industrialization, high O₃ mixing ratios were frequently
48 observed in the Pearl River Delta region (e.g., Zheng et al., 2010; Li et al., 2014; Wang et al., 2017).



49 Many previous studies have shown that photochemical O₃ formation was generally VOCs-limited in the
50 PRD region, and suggested that the reduction of VOC emission could effectively alleviate photochemical
51 O₃ formation (Guo et al., 2017). Therefore, source identification and quantification of VOCs are
52 prerequisites for the formulation and implementation of the most effective control measures of
53 photochemical pollution in the PRD region. Indeed, many efforts have been made to perform the source
54 apportionments of VOCs in this region by using different methods, including tunnel measurements,
55 receptor models, emission-based measurements, and emission inventory. Ho et al. (2009) quantified the
56 emission factors of 92 VOCs from gasoline, diesel, and LPG vehicles from a tunnel study in Hong Kong.
57 Guo et al. (2011b) and Zheng et al. (2013) characterized the source profiles of VOCs emitted from
58 industrial and vehicular sectors through samples collected directly from the plumes of the above sources.
59 These emission-based measurements provided clear attributions of VOCs from different sources and
60 emission factors for the emission-inventory to estimate the total amount of VOCs emitted from those
61 sources. In particular, Zheng et al. (2009) and Ou et al. (2015b) established a specific VOC emission
62 inventory to estimate the abundance of VOCs and to provide input data for different air quality models.
63 The inventory was applied to quantify the strength of vehicular emissions, solvent usage, and biogenic
64 emissions in the PRD.

65 In contrast to emission inventory, which estimates the emission strength based on emission factors and
66 emission activity, receptor models are useful for source apportionment of VOCs without any prior
67 knowledge of the emissions. As a widely used receptor model, positive matrix factorization (PMF) has
68 been employed in the source apportionment of VOCs in the PRD region (Guo et al., 2011a; Ling et al.,
69 2011; Lau et al., 2010; Ou et al., 2015a). For example, Ling et al. (2011) identified 10 sources of VOCs
70 at a receptor site in the PRD region and concluded that solvent usage and vehicular exhaust were the most
71 significant sources with average contributions of 51% and 37%, respectively. Results from source
72 apportionment using the PMF model demonstrated the important roles of vehicular emissions in ambient
73 VOCs in urban ($65 \pm 36\%$) and suburban ($50 \pm 28\%$ and $53 \pm 41\%$) environments of Hong Kong (Lau et



74 al., 2010; Ou et al., 2015a). However, uncertainties existed in the PMF analysis due to the assumption of
75 mass conservation during the transport of pollutants from emissions to the receptor site. To investigate
76 the influence of photochemical processes on the factorization of VOCs by the PMF model, Yuan et al.
77 (2012b) applied a photochemical age-based parameterization method to analyze the measured VOC data
78 at an urban site in Beijing. They found that the PMF-resolved factors were influenced by VOCs from a
79 common source at different stages of the photochemical processing, thus the independent source could
80 not be clearly identified. The results further suggested that when using the PMF model for VOC source
81 apportionments, it is necessary to assess if photochemical processing could influence the source
82 signatures of VOCs at the receptor site. Although many previous studies reported source apportionment
83 of VOCs in the PRD region using the PMF model, they did not take the influence of photochemical
84 processing into account, leading possibly to uncertainties in identifying and quantifying the source
85 attribution of VOCs.

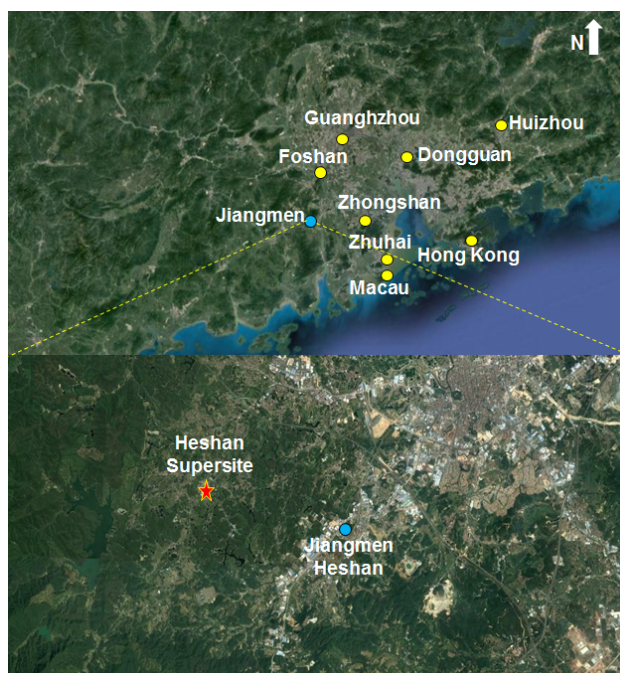
86 In this study, the PMF model coupled with a photochemical-age-based parameterization method was
87 applied to the continuous real-time VOCs data from an intensive field campaign at a receptor site in PRD.
88 The model provides a more detailed and accurate description of the source characteristics of VOCs in the
89 PRD region. Furthermore, the contribution of different sources of VOCs to the photochemical O₃
90 formation and the sensitivity of ozone and its precursors were evaluated through a photochemical box
91 model coupled with the master chemical mechanism. Our results could provide valuable information,
92 facilitating local and regional policy-makers for proposing appropriate strategies and effective control
93 measures of VOCs and photochemical pollution.



94 2 Methodology

95 2.1 Measurements

96 The field measurement was conducted at the Heshan (HS) Atmospheric Supersite (22.728°N, 112.929°E,
97 at an altitude of 60 m) in the western PRD region from October 22 to November 20, 2014. Figure 1 shows
98 the surrounding environment at the sampling site. A detailed description of the Heshan site can be found
99 in previous studies (Zhou et al., 2013, 2014). Briefly, the site is located in a rural area of the PRD region,
00 about 50-80 km northeast of the urban central cities (i.e., Guangzhou and Foshan) of the PRD region. In
01 addition to local emissions, the abundances of air pollutants at the HS during autumn and winter seasons
02 are frequently affected by the outflow of air masses from the central cities, thus this site can be used as a
03 representative of regional emissions in the PRD region (Zhou et al., 2014).



04



05 Figure 1. The sampling site and its surrounding environment in the Pearl River Delta region (top panel: overview of the
06 site location; bottom panel: zoomed-in view, red star denotes the site location)

07

08 An automated online gas chromatography-flame ionization detector (GC-FID) system measured hourly
09 concentrations of 58 VOC species at the site from October 22 to November 20, 2014. Detailed
10 descriptions of the configuration of the GC-FID system, the detection limits, and precision of VOCs can
11 be found elsewhere (Wang et al., 2008; Zhang et al., 2008a; Ling et al., 2017). Air-quality related trace
12 gases, including O₃, NO-NO₂-NO_x, CO, and SO₂, together with meteorological data, *i.e.*, temperature,
13 solar radiation, precipitation, relative humidity, wind speed, and wind direction were continuously
14 measured by the Guangdong Environmental Monitoring Center.

15 2.2 Positive matrix factorization (PMF) model

16 The Positive Matrix Factorization (PMF) (US Environmental Protection Agency (USEPA) version 5.0)
17 model was applied to the observed data for source apportionments of the VOCs. The PMF model is a
18 multivariate factor analysis tool that decomposes a matrix of speciated sample data into two matrices,
19 factor contributions, and factor profiles, which can be interpreted by an analyst as to explore the source
20 types and their contributions based on the measured data at the receptor site (Paatero and Tapper, 1994;
21 Paatero, 1997). It could be simplified as

$$22 \quad x_{ij} = \sum_{k=1}^p g_{ik} f_{kj} + e_{ij}, \quad (1)$$

23 where x_{ij} is the j th species concentration measured in the i th sample, g_{ik} the species contribution of the
24 k th source to the i th sample, f_{kj} the j th species fraction from the k th source, e_{ij} the residual for each
25 species, and p the total number of independent sources (Paatero, 1997). The model could provide the
26 number of emission sources (p) and the distributed profiles (f) of each species in the individual source
27 after simulation.



28 The description of the model input was provided elsewhere (Guo et al., 2011a). In this study, the selection
29 of species for the model input followed several criteria: 1) The chosen species had relatively high
30 concentrations and/or were typical tracers for specific emissions. 2) Species with low abundance and/or
31 high uncertainties were excluded, *i.e.*, *cis*-2-pentene, diphenyl methane, and 1,3-diethylbenzene, because
32 more than a quarter of the samples for those species were below the detection limit. 3) Species related to
33 biogenic emissions, *i.e.*, isoprene and α/β -pinene, were excluded as this study focused on the source
34 characteristics of anthropogenic emissions in the PRD region (Fuentes et al., 1996; Sanadze, 2004). A
35 total of 49 species, including 47 VOCs, MTBE (methyl tert-butyl ether), and acetonitrile (ACN) were
36 selected for the input data.

37 For the PMF modeling run, different numbers of factors were tested and an optimal number of factors
38 was determined based on both a good fit to the data and the most meaningful results. The uncertainty for
39 each species was determined to be sum of 10% of the VOC concentration and two times the detection
40 limit of the species (Paatero, 2000a; Lau et al., 2010). Concentrations below the detection limit were
41 replaced with half of the detection limit and their uncertainties were set to be 5/6 of the detection limit.
42 Missing concentrations were replaced by the geometric mean of the measured values and their
43 corresponding uncertainties were set to be four times the geometric mean values (Paatero, 2000b).

44 **2.3 PBM-MCM model**

45 The photochemical box model coupled with the master chemical mechanism (PBM-MCM) was applied
46 to quantify the contributions of VOC emission sources to in-situ O₃ formation. The PBM-MCM model
47 uses the concentrations of VOCs and trace gases, and the meteorological data as input to simulate the
48 total amount of photochemical O₃ formation at the site based on the master chemical mechanism (version
49 3.2), which consists of 5900 chemical species and 16500 reactions. Note that the physical processes,
50 including horizontal and vertical transport, were not considered in the model. Details of the model setup
51 and configuration can be found in previous studies (Saunders et al., 2003; Lam et al., 2013). In this study,



52 the hourly data of VOCs, five trace gases (i.e., O₃, NO, NO₂, CO, and SO₂) and two meteorological
53 parameters (i.e., temperature and relative humidity) measured during the campaign were used as model
54 input.

55 In addition, the PBM-MCM model can be used to assess the sensitivity of O₃ photochemical production
56 to the changes in the concentrations of its precursors by calculating the relative incremental reactivity
57 (RIR) without a detailed or accurate knowledge of these emissions (Carter and Atkinson, 1989; Cardelino
58 and Chameides, 1995). The RIR is defined as the percent change in O₃ production per percent change in
59 the precursors. The RIR of a specific precursor X at site S is given by

$$60 \quad RIR^S(X) = \frac{[P_{O_3-NO}^S(X) - P_{O_3-NO}^S(X-\Delta X)] / P_{O_3-NO}^S(X)}{\Delta S(X) / S(X)} \quad (2)$$

61 where $S(X)$ represents the measured concentration of precursor X , including the amounts emitted at the
62 site and those transported to the site and ΔX is the change in the concentration of precursor X caused by
63 a hypothetical change $\Delta S(X)$ (10% $S(X)$ in this study). Here, $P_{O_3-NO}^S$ represents the O₃ formation
64 potential, which is the net O₃ production and NO consumed during the evaluation period and can be
65 calculated by the output from the PBM-MCM. A large positive RIR value of a specific precursor suggests
66 that the O₃ production could be decreased significantly if the emissions of this precursor were controlled.

67 In addition, the average RIR function of precursor X can be calculated from

$$68 \quad \overline{RIR}(X) = \frac{\sum_1^N [RIR^S(X) P_{O_3-NO}^S(X)]}{\sum_1^N P_{O_3-NO}^S(X)} \quad (3)$$

69 where N means the number of days simulated.

70 In addition, considering both the reactivity and abundance of VOC species in different sources, the
71 relative contributions of the precursor X can be calculated by (Ling et al., 2011; Ling and Guo, 2014).

$$72 \quad Contribution(X) = \frac{\overline{RIR}(X) \times conc(X)}{\sum [\overline{RIR}(X) \times conc(X)]} \times 100\% \quad (4)$$

73 where $conc(X)$ was obtained from the measurement and PMF resolutions.



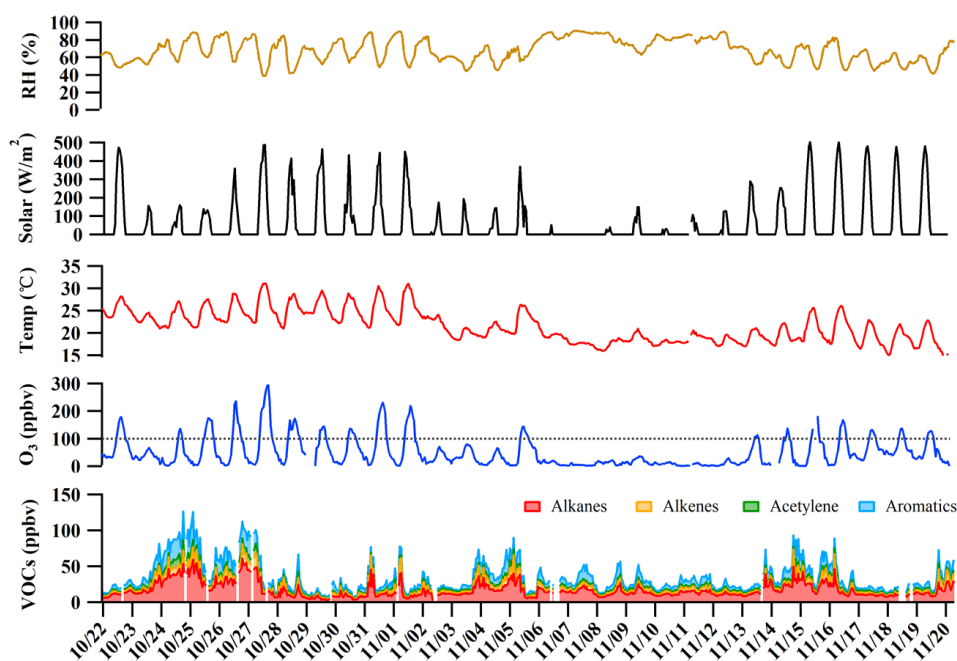
74 **3 Results and discussion**

75 **3.1 General statistics**

76 Figure 2 shows the time series of O₃ and total VOCs (TVOCs), as well as meteorological parameters (i.e.,
77 temperature, relative humidity) observed at Heshan site from 22 October to 20 November. It was found
78 that two major episodes of high O₃ mixing ratios (maximum hourly-averaged mixing ratio > 100 ppbv,
79 China II Standard) appeared during 24 October ~ 01 November and 13~19 November, respectively.
80 Consistent with higher O₃ levels, the mixing ratios of TVOCs in O₃ episode days were higher, with the
81 average values of 38 ± 3 ppbv and 30 ± 2 ppbv (mean \pm 95% intervals) observed during O₃ episode and
82 non-episode days, respectively, indicating that O₃ formation at Heshan site was probably VOC-limited.
83 The measured 58 VOC species included 30 alkanes, 10 alkenes, 17 aromatics, and acetylene. Table 1
84 summarizes the average mixing ratios of the major VOC groups measured at the site from 22 October to
85 20 November, 2014. The average mixing ratio of total VOCs was 34 ± 3 ppbv, with the highest
86 contributions from alkanes (17 ± 2 ppbv, 49%), followed by aromatics (9 ± 1 ppbv, 26%), alkenes (5 ± 1
87 ppbv, 15 %) and acetylene (3 ± 1 ppbv, 10%). This is consistent with previous measurements in this
88 region (Guo et al., 2011a; Yuan et al., 2012a; Zou et al., 2015). The VOC mixing ratio at the Heshan site
89 was similar to that in urban Shanghai and Beijing, with a range of 30.3-38.7 ppbv (Geng et al., 2009; Cai
90 et al., 2010) and 29.4-43.4 ppbv (Song et al., 2007; Duan et al., 2008; Shao et al., 2009; Li et al., 2015),
91 respectively. However, it was much higher than that in background areas of the North China Plain region,
92 Yangtze River Delta region, and PRD (< 20 ppbv) (Tang et al., 2009; Yuan et al., 2012b; Zhu et al., 2016).
93 The most abundant VOC species was ethane (3.86 ± 0.10 ppbv), followed by toluene (3.74 ± 0.22 ppbv),
94 acetylene (3.42 ± 0.17 ppbv), propane (3.01 ± 0.14 ppbv), and ethene (2.94 ± 0.25 ppbv). The composition
95 and the variations of VOCs suggest that the air masses arriving at the Heshan site may be through
96 photochemical processing. In addition, incomplete combustion was likely to be the dominant source of
97 VOCs at this site (Yuan et al., 2012a; Zhang et al., 2014; Yang et al., 2017), because typical tracers of



98 incomplete combustion (i.e., ethane, acetylene, ethene, and propane) were present with high
99 concentrations due to relatively lower photochemical reactivity of alkane (i.e., ethane and propane) than
00 other VOCs. Indeed, the average diurnal variations of VOCs (Figure 3) presented relative higher mixing
01 ratios during the early morning and from the evening to midnight, which may be related to elevated traffic
02 emissions during rush hours and the constrained mixing height (Yuan et al., 2009). On the other hand, the
03 mixing ratios of VOCs started to decrease at 0900 LT (local time) and presented a broad trough during
04 daytime hours (0900-1900 LT), which were probably due to strong photochemical reactions, increased
05 mixing height and/or less VOC emissions (Yuan et al., 2009; Lau et al., 2010).



06

07

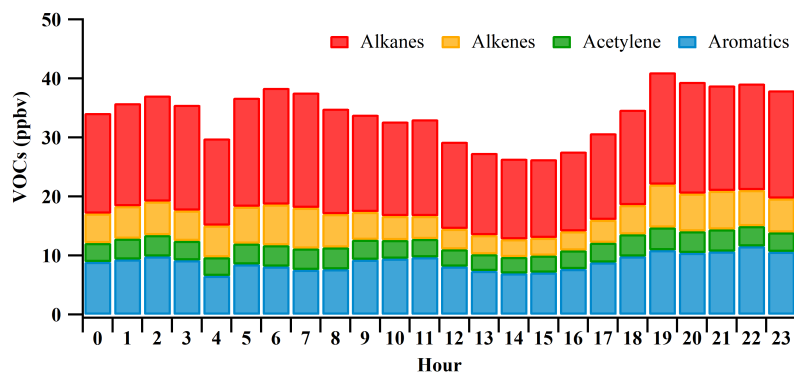
Figure 2. Time series of O₃, VOCs, and meteorological parameters observed at Heshan site

08



09 Table 1. Average, range, and standard deviation of concentrations for the eight most abundant VOCs measured at the
 10 Heshan site, together with a sum of the mixing ratios for each hydrocarbon category (i.e., alkanes, aromatics, and alkenes)

| Species | Average \pm standard deviation (ppbv) | Range (ppbv) |
|--------------------|---|--------------|
| Ethane | 3.86 ± 1.34 | 1.08 - 10.44 |
| Toluene | 3.74 ± 2.89 | 0.56 - 15.80 |
| acetylene | 3.42 ± 2.33 | 0.11 - 28.22 |
| Propane | 3.01 ± 1.82 | 0.45 - 10.70 |
| Ethene | 2.94 ± 3.34 | 0.37 - 64.56 |
| <i>i</i> -Pentane | 1.90 ± 2.20 | 0.22 - 16.16 |
| <i>n</i> -Butane | 1.85 ± 1.28 | 0.20 - 10.10 |
| <i>m/p</i> -Xylene | 1.62 ± 1.44 | 0.17 - 12.74 |
| Alkanes | 17.04 ± 10.64 | 2.04 - 61.01 |
| Aromatics | 9.07 ± 7.01 | 1.46 - 40.12 |
| Alkenes | 5.29 ± 5.01 | 0.67 - 77.39 |



11

12

Figure 3. Diurnal variations of VOCs observed at Heshan site

13 3.2 Sources of VOCs

14 3.2.1 The influences of photochemical processing on VOCs concentration

15 To investigate the source attributions of VOCs, the PMF model was applied to the observed
 16 concentrations of VOCs at the Heshan site. As mentioned above, to more accurately identify and quantify



17 the source contributions, it is necessary to evaluate whether the photochemical processing could influence
18 the source signatures of VOCs.

19 Correlation analysis between two VOC species from the same emissions with different photochemical
20 reactivity, *i.e.*, propane vs butanes and ethylbenzene vs xylenes, has been widely used in previous studies
21 to evaluate the photochemistry impacts (Ling et al., 2011). If the two species are involved in
22 photochemical reactions, their correlation will weaken due to their different reactivity. In the present study,
23 excellent correlation was found for ethylbenzene vs *o*-xylene ($R^2 = 0.95$, $p < 0.01$) and propane vs *i*-
24 butane ($R^2 = 0.91$, $p < 0.01$) (figure not shown), indicating the insignificant influence of photochemical
25 processing on the correlations and clear source signatures for the selected species.

26 To evaluate further the influence of photochemical processing on the observed levels, a photochemical-
27 aged-based parameterization method was used to estimate the initial concentrations of VOCs after
28 emissions (Eq. (5)). This method was first introduced by de Gouw et al. (2005) and was applied to VOC
29 measured data in different environments (Liu et al., 2009; Shao et al., 2009; Yuan et al., 2012b).

30 Through the photochemical-aged-based parameterization method, photochemical age, representing the
31 photochemical processing time, could be calculated by the ratio between the concentrations of two VOCs
32 with relatively strong correlation and different OH reaction rates, *i.e.*, the ratio of ethylbenzene and *m/p*-
33 xylene. In this study, high correlation was found between ethylbenzene and *m/p*-xylene ($R^2 = 0.96$, $p <$
34 0.01). Furthermore, the OH reaction rate constants for the above species were 7.10×10^{-12} (ethylbenzene),
35 1.90×10^{-11} (*m/p*-xylene, obtained from the average OH reaction rate constants of *m*- and *p*-xylene)
36 $\text{cm}^3 \cdot \text{molecule}^{-1} \cdot \text{s}^{-1}$, respectively. It has been demonstrated that ratios of above species could be used to
37 estimate the effect of photochemical processing on VOC variations (Shiu et al., 2007; Shao et al., 2009;
38 Chang et al., 2010). The OH exposure ($[\text{OH}]\Delta t$) is calculated and used to represent photochemical age,
39 as $[\text{OH}]$ and Δt always appear together in the parameterization equation (Jimenez et al., 2009). The OH
40 exposure is calculated from the ratio of VOCs concentrations by



$$[OH]\Delta t = \frac{1}{(k_E - k_X)} \times \left[\ln \frac{[E]}{[X]} \Big|_{t=0} - \ln \frac{[E]}{[X]} \right] \quad (5)$$

The $[OH]$ term represents the concentration of the OH radical and its reaction time Δt for VOCs between the emission sources and the observation site. The parameters k_E and k_X are the reaction rate constants of ethylbenzene and *m/p*-xylene, 7.10×10^{-12} and 1.90×10^{-11} $\text{cm}^3 \cdot \text{molecule}^{-1} \cdot \text{s}^{-1}$, respectively (Atkinson et al., 2006). $\frac{[E]}{[X]}$ is the average measured concentration ratio of ethylbenzene to *m/p*-xylene. $\frac{[E]}{[X]} \Big|_{t=0}$ is the initial concentration ratio of ethylbenzene to *m/p*-xylene.

In the present study, the initial concentration ratio of ethylbenzene to *m/p*-xylene ($\frac{[E]}{[X]} \Big|_{t=0}$) is calculated to be 0.62 using the methods suggested by Yuan et al. (2012b) and Shao et al. (2009), consistent with those calculated at other urban and rural environments (Shao et al., 2009), and the OH exposure ($[OH]\Delta t$) calculated by Eq. (5) was 6.47×10^9 $\text{molecule} \cdot \text{cm}^{-3} \cdot \text{s}$.

On the other hand, the initial concentration of VOCs could be described by

$$[VOC]_{\text{initial}} = [VOC]_{\text{measured}} \times \exp(-k_{NMHC} \cdot [OH]\Delta t) \quad (6)$$

Here, $[VOC]_{\text{initial}}$ and $[VOC]_{\text{measured}}$ are the initial and measured concentration of particular VOC, respectively. k_{VOC} is the reaction rate constant of the specific VOC.

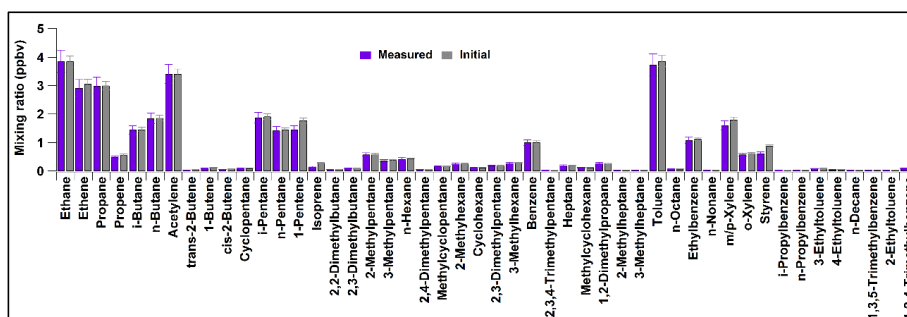


Figure 4. Average measured and initial concentrations of VOCs



58 Figure 4 shows the comparison between the observed levels and the initial concentrations of VOCs at the
59 Heshan site. In general, the variations between the observed levels and the initial concentrations of VOCs
60 were small for most of the VOC species, with the OH reaction rate $< 5.64 \times 10^{-11} \text{ cm}^3 \cdot \text{molecule}^{-1} \cdot \text{s}^{-1}$, and
61 the ratio of initial/observed concentrations ranging from 1.00-1.23. However, for those species with
62 relatively higher photochemical reactivity (with the OH reaction rate ranging from 5.64×10^{-11} - 6.40×10^{-11}
63 $\text{cm}^3 \cdot \text{molecule}^{-1} \cdot \text{s}^{-1}$), the initial concentrations were 1.44-1.51 times of the observed levels. It should be
64 noted that these relatively higher reactive species only accounted for a small fraction of the concentrations
65 and the ozone formation potential (OFP) of all the observed VOCs due to their relatively lower abundance
66 (data not shown).

67 Therefore, to consider the influence of photochemical processing on source apportionment results, the
68 concentrations for the species with relatively higher reactivity (the ratio of initial/observed concentrations $>$
69 1.3, *i.e.*, *trans*-2-butene, *cis*-2-butene, styrene, and 1,3,5-trimethylbenzene) were compensated by the
70 difference between observed levels and initial concentrations. They were further used as input to the PMF
71 model, together with the observed concentrations of rest species to investigate the source attributions of
72 VOCs at the Heshan site in the following section.

73 3.2.2 Source apportionments of VOCs

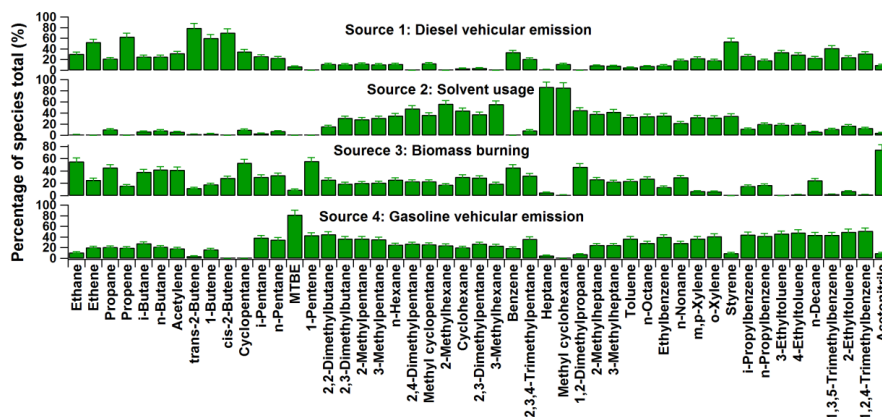
74 In this study, the data matrix for PMF model was composed of 682 samples and 47 VOCs together with
75 ACN and MTBE. The solution of four factors was obtained. Figure 5 presents the source profiles (in
76 percentages of species total) extracted from the PMF model, while Figure 6 presents the relative
77 contributions of different sources to ambient VOCs at the Heshan site. It was found that factor 1 and 4
78 were both associated with high percentages of aromatics. In addition to the solvent usage, aromatics were
79 mainly related to vehicle emissions in the PRD region (Zhang et al., 2013; Ou et al., 2014). The relatively
80 higher loadings of C₂-C₄ alkenes in factor 1 suggest that this source was mainly related to diesel vehicular
81 emission (Guo et al., 2011a; Ou et al., 2014), which accounts for about $25 \pm 3\%$ (mean \pm 95% intervals)



82 of the total observed VOCs. On the other hand, factor 4 was characterized by high levels of *n*/*i*-pentane
83 and MTBE, the typical tracers for gasoline vehicular emissions (Song et al., 2006; Ho et al., 2009; Ou et
84 al., 2014). As such, factor 4 was assigned to gasoline vehicular emission and its contribution to the
85 observed VOCs was $33 \pm 5\%$. Factor 2 was characterized by high percentages of C₆-C₇ alkanes and certain
86 amounts of aromatics, while the contributions of other combustion tracers were insignificant in this factor,
87 suggesting that this factor was related to solvent usage. It is consistent with previous studies that aromatics
88 and C₆-C₇ could be used as solvents in the printing and paint industry (He et al., 2002, Chan et al., 2006;
89 Liu et al., 2008). $18 \pm 2\%$ of the observed VOCs, were identified to be associated with solvent use. Factor
90 3 was represented by high percentages of ethane (~65%), acetylene (~51%), benzene (~52%), and ethene
91 (~ 31%), together with some C₃-C₅ alkanes and alkenes, which are typically tracers of incomplete
92 combustion such as vehicular exhaust and biomass burning (Nelson et al., 1984; Wadden et al., 1986;
93 Blake et al., 1994; Rudolph, 1995; Guo et al., 2011a, 2011b). The high percentage of acetonitrile in factor
94 3 suggests that this factor was associated with biomass burning (Holzinger et al., 1999; Yuan et al., 2010),
95 which was responsible for $24 \pm 3\%$ of the observed VOCs. Figure 7 shows the diurnal variations of VOCs
96 emitted from different sources extracted from PMF. Different diurnal patterns were found for different
97 sources, which may be related to the variations in emission strength, the concentrations of species in
98 different source profiles, as well as the influence of mixing height. For example, relatively higher levels
99 were found for the diesel and gasoline vehicular emissions in the early morning and in the evening,
00 corresponding well with traffic emissions during rush hours, while a broad peak during daytime hours
01 may be related to the increased mixing height and photochemical loss, and decreased emission strength
02 (Zheng et al., 2010; Yuan et al., 2009). Different from vehicular emissions, the concentrations of solvent
03 usage started to increase in the early morning and reached maximum value at noon, and then decreased
04 gradually and presented a broad peak until midnight. The increased levels of solvent usage from early
05 morning to midday was associated with the increased emissions from human production activities and the
06 increased temperature which would accelerate VOCs evaporated during the use of solvent. The diurnal



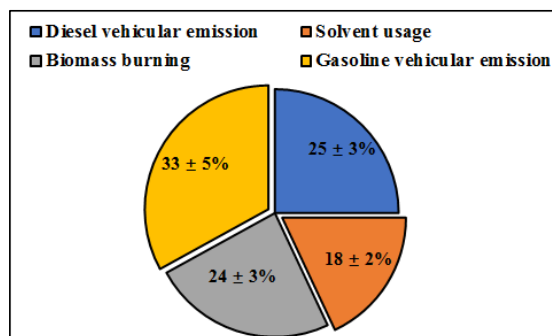
07 variations of biomass burning were much weaker compared with other sources, with peak values occurred
 08 in the early morning, which was consistent with the diurnal patterns of plumes of biomass burning at
 09 Heshan site (Yuan et al., 2010).



10

11

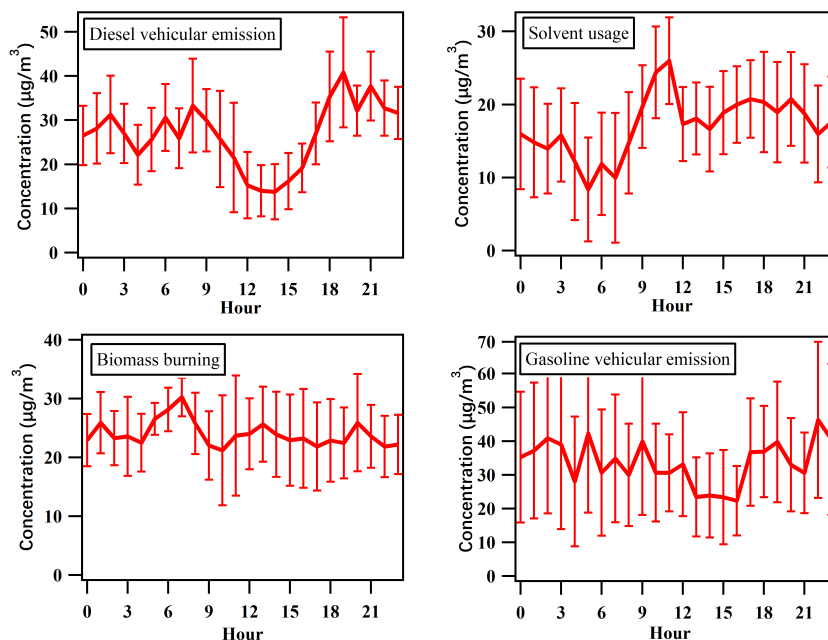
Figure 5. Factor profile (in percentage of species total) attributed from PMF



12

13

Figure 6. Contributions of different sources to ambient VOCs extracted from PMF



14

15

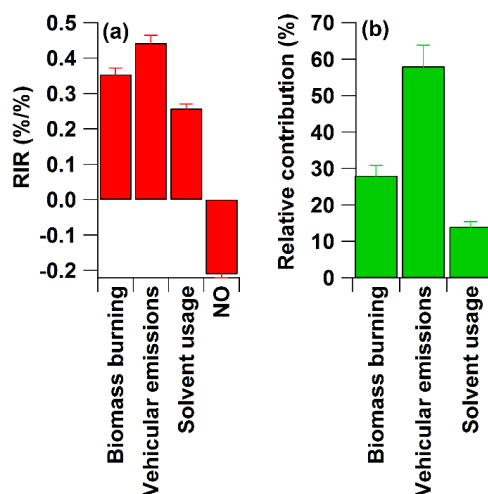
Figure 7. Diurnal variations of VOCs emitted from different sources extracted from PMF

16 3.3 The contributions of VOCs sources to ozone photochemical formation

17 To evaluate the roles of the different VOCs emissions for O₃ formation, we applied the PBM-MCM model
18 to the PMF-extracted VOC concentrations. Figure 8(a) shows the average RIR values of different VOC
19 sources and NO, together with the contributions of different VOC sources to photochemical O₃ formation.
20 The average RIR values of various VOC sources were positive, while that of NO was negative, suggesting
21 that O₃ formation at Heshan site was located in the VOC-limited regime. Among the four main
22 anthropogenic sources of VOCs, relative higher average RIR values of vehicular emissions and biomass
23 burning than that of solvent usage were found. Furthermore, considering both the reactivity and
24 abundance of VOCs in different sources, the relative contributions of the four anthropogenic sources were



25 calculated by Eq. (3) and the results are shown in Figure 8(b). It shows that the vehicular emissions,
26 including diesel and gasoline vehicular emissions, made the most important contributions to
27 photochemical O₃ production, with an average percentage of 58%, followed by biomass burning (28%)
28 and solvent usage (14%), suggesting that controlling vehicular emissions and biomass burning could be
29 more effective way for reduction of O₃ pollution at Heshan.



30

31 Figure 8. The average RIR values of VOC sources and NO, together with the contributions of different VOC sources to
32 photochemical O₃ formation at Heshan

33 3.4 Improvement for the reduction of VOCs and NO_x to photochemical O₃ formation

34 3.4.1 Sensitivity analysis of ozone formation

35 Changes in the concentrations of VOCs and NO_x will affect O₃ formation, leading to a great variation of
36 the O₃ concentration, which can be illustrated from the ozone isopleth plot. The PBM-MCM model was
37 employed to perform a sensitivity study based on the average diurnal variations of the observed air
38 pollutants (*i.e.*, 58 VOCs, O₃, NO, NO₂, CO, and SO₂.) at the site. We followed the procedures suggested

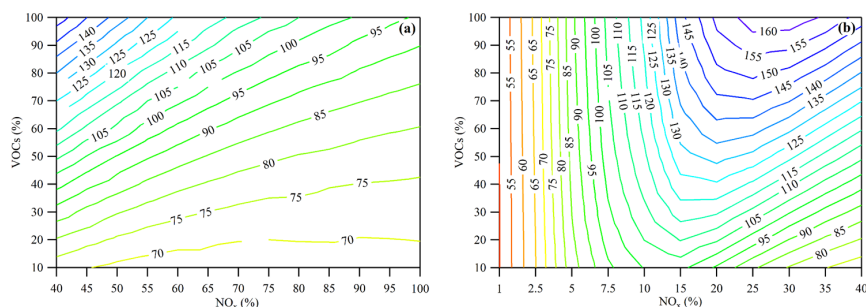


39 by Lyu et al. (2016) to investigate the O₃ variations related to the changes of precursors. A total of 520
40 reduction scenarios (26 NO_x × 20 VOCs) were simulated and the maximum O₃ value in each scenario
41 was selected. Figure 9 shows the obtained ozone isopleth based on the observed levels of VOCs and NO_x
42 at Heshan site.

43 The two ozone isopleths (Figure 9(a) and (b)) show distinct characteristics of O₃ variations. For a 0-60%
44 reduction of NO_x (corresponding to 40-100% of original NO_x), the O₃ mixing ratio decreases significantly
45 with VOCs for a certain NO_x condition but increases slightly with decreasing NO_x for a fixed mixing ratio
46 of VOCs (Figure 9(a)). This clearly indicates a VOC-limited regime for O₃ formation in this region and
47 is consistent with previous results found in the urban, suburban, and even some rural environments, as
48 well as the downwind site of the PRD region (Zhang et al., 2008b; Cheng et al., 2010; Ling et al., 2011;
49 Zheng et al., 2013; Ling and Guo, 2014). However, it is different from the results found in the northern
50 rural areas of the PRD region based on the measured ratios of O₃/NO_x (Zheng et al., 2010). Here, we
51 introduce the absolute value of RIR (|RIR|) to evaluate the sensitivity of the O₃ formation to VOCs and
52 NO_x. It turns out that the |RIR| decreases with VOCs for a fixed NO_x, while it fluctuates at first and then
53 increases with decreasing NO_x for a fixed VOCs. This implies that the efficiency of O₃ reduction by
54 cutting down VOC emissions alone would decrease gradually (data not shown) and we may need to pay
55 attention to the counter effects caused by decreasing NO_x. For NO_x reduction to 0-40% of the original
56 level, a clear ridge can be seen (Figure 9(b)), dividing the isopleth into two parts: VOCs-limited (right)
57 and NO_x-limited (left). In the VOCs-limited regime, the effects of both VOCs and NO_x on O₃ formation
58 are linear, and the ozone concentration is apparently proportional to the amounts of VOCs (and NO_x): the
59 higher the VOCs mixing ratio (or the lower the NO_x), the higher the O₃ concentration. On the other side
60 of the ridge, for the reduced NO_x to 7.5-15% of original mixing ratio, O₃ concentration decreases with
61 NO_x concentration, but VOCs decrease would lead to O₃ increase. Ideally, the NO_x reduction to its 1-
62 7.5%, a regime with “pure” NO_x-limited would occur, where ozone formation is solely controlled by the



- 63 NO_x concentrations and insensitive to the change of VOCs. The reduction of NO_x emissions in this case
64 will be the most effective measure for mitigating ozone production.



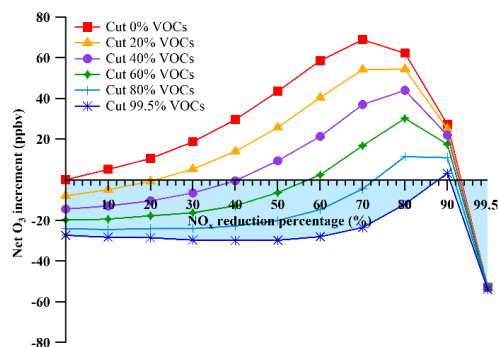
- 65
66 Figure 9. The ozone isopleth in term of percentage changes of VOCs and NO_x: the percentage change of NO_x from 0 to
67 60% (a) and from 60 to 99% (b). The ozone mixing ratios are in ppbv. The horizontal and vertical axes correspond to
68 the percentage of the measured average mixing ratios of NO_x and VOCs, respectively.

69 3.4.2 Development of the most optimum control measures on both VOCs and NO_x

- 70 Though it was found that the O₃ formation was located in the VOCs-limited regime at the Heshan site
71 (with 100% of NO_x and VOCs as input), it is unknown how much VOCs should be controlled for the
72 most efficient O₃ reduction, especially in society where VOCs and NO_x frequently are controlled
73 simultaneously. To achieve this goal and provide detailed information about the amounts of VOCs and
74 NO_x that need to be controlled, we simulated the net O₃ increment (the total increase of average O₃
75 concentrations when both VOCs and NO_x are reduced) with the reduction of both VOCs and NO_x. This
76 is shown in Figure 10. The horizontal and vertical axis corresponds, respectively, to the reduction
77 percentages of NO_x (e.g., 10% means that the mixing ratios of NO_x were reduced by 10%) and the net
78 increments of O₃ (positive and negative values represent the increase and decrease of O₃ compared to the
79 base case with no reduction of VOCs and NO_x, respectively). The different curves correspond to scenarios
80 with different cutting percentages of VOCs. It shows that the net O₃ increments increased as the reduction
81 percentages of NO_x increased from 0 to 70% regardless of the reduction of VOCs, while the net O₃



82 increment decreased gradually, starting from the NO_x reduction percentage of $\sim 70\%$. However, an
83 optimum control measure for VOCs and NO_x was that when this control measure was conducted, the O_3
84 mixing ratios would be reduced or at least the O_3 mixing ratios would not increase (*i.e.*, the value of the
85 net O_3 increment was less than or equal to zero, the highlighted area in Figure 10). It was found that when
86 the mixing ratios of VOCs were reduced from 0 to 99.5%, the appropriate reduction percentages of NO_x
87 should be located between 0 and 88% or between 90 and 99.5% for zero O_3 increment. However, it was
88 interesting to find that when the reduction percentages of NO_x ranged from 90 to 99.5%, the O_3 formation
89 reduced with the reduction of NO_x regardless of the reduction of VOCs, though reducing NO_x by 90~99.5%
90 is probably unrealistic. Therefore, this section only focused on the range of 0~88% of NO_x reduction for
91 devising optimum controlling measures of VOCs and NO_x . It was determined that when the reduction
92 percentages of NO_x ranged from 0 to 88%, the minimum abatement ratio of VOCs/ NO_x for zero O_3
93 increment changed from ~ 1 to 1.1 (*i.e.*, the cutting ratios of VOCs/ NO_x at the intersections of the curves
94 and the horizontal axis). This suggests that the abatement ratio of VOCs/ NO_x should be more than 1.1 to
95 prevent the increase of the O_3 levels at Heshan.



96

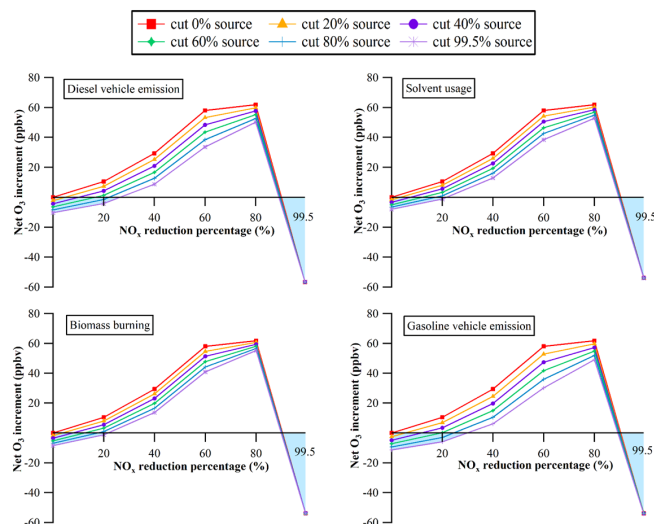
97 Figure 10. Net O_3 increment as function of the reduction percentages of NO_x and VOCs. The highlighted area represents98 zero O_3 increment

99



00 Furthermore, to determine the appropriate cutting ratios of the individual source of VOCs vs NO_x when
01 both VOC sources and NO_x were reduced, O_3 -VOC sources- NO_x sensitivity analysis was conducted. The
02 net O_3 increments as a function of the reduction percentages of NO_x for the individual VOC source are
03 shown in Fig. 11. For different VOC sources, the patterns of the net O_3 increment as a function of different
04 NO_x reductions are similar, with O_3 increments increased when the mixing ratios of NO_x was reduced by
05 0~80% and decreased with the reduction percentages of NO_x ranging from 80 to 99.5%. It was found that
06 when the cutting percentages of VOCs increased from 0 to 99.5%, the appropriate reduction percentages
07 of NO_x for zero O_3 increment were located in the ranges of 0~30% and 90~99.5%. It was interesting to
08 find that when the reduction percentages of NO_x ranged from 90 to 99.5%, the O_3 formation reduced with
09 the reduction of NO_x regardless of the reduction of VOCs, though reducing NO_x by 90~99.5% is probably
10 unrealistic in the near future. Therefore, here we only focus on the range of 0~30% of NO_x reduction to
11 provide appropriate reduction ratios for devising optimum controlling measures of VOCs and NO_x .

12 It was found that the specific appropriate reduction percentages of NO_x for zero O_3 increment was 0~27%,
13 0~22%, 0~22%, and 0~30% for diesel vehicle emission, solvent usage, biomass burning, and gasoline
14 vehicular emission, respectively, while the abatement ratio of individual sources of VOC vs NO_x should
15 be more than 3.8, 4.6, 4.6, and 3.3 for diesel vehicular emission, solvent usage, biomass burning, and
16 gasoline vehicular emission, respectively. For example, if the mixing ratios of NO_x were reduced by 10%,
17 more than 38% of diesel vehicular emission, 46% of solvent usage or biomass burning, or 33% of gasoline
18 vehicular emission needs to be cut to prevent increase of O_3 levels at Heshan. Furthermore, the above
19 ratios demonstrate that reducing VOCs from gasoline vehicular emission has the highest efficiency for
20 both reductions of VOCs and NO_x without increasing O_3 levels, followed by diesel vehicular emission,
21 biomass burning, and solvent usage.



22

23 Figure 11. Net O₃ increment as a function of the reduction percentages of NO_x for individual sources of
24 VOC. The highlighted area represents zero O₃ increment

25 4 Conclusion

26 The PRD region has long been facing severe photochemical air pollution, and VOCs has been the limiting
27 factor of ozone formation in this region. To better understand the contribution of different anthropogenic
28 VOCs to the ozone formation in this region, we performed in-depth analysis on the data of intensive
29 measurement of VOCs and related species conducted at a downwind rural site (the HeShan site) of the
30 PRD region during October to November of 2014. Overall the mixing ratio of total measured VOCs was
31 high and similar to other urban cluster regions. By using the PMF model with consideration of
32 photochemical processing effects, four anthropogenic emissions sources were identified. The vehicular
33 emission was the most important source of VOCs and also the major contribution to O₃ formation at
34 Heshan site, followed by biomass burning. The PBM-MCM model analysis confirms that the ozone
35 formation at Heshan was VOC-limited, and the regime would not transform until the NO_x is reduced to ≤



36 25% of the current concentration. The O₃-VOCs-NO_x sensitivity analysis in the whole air suggested
37 that >1.1 of the abatement ratio of VOCs/NO_x was the most appropriate abatement ratio when both the
38 VOC and NO_x were reduced to prevent net O₃ increment. Furthermore, O₃-VOC sources-NO_x sensitivity
39 analysis suggested that the cutting ratios of individual source of VOC vs NO_x should be more than 3.8,
40 4.6, 4.6, and 3.3 for diesel vehicular emission, solvent usage, biomass burning, and gasoline vehicular
41 emission, respectively, for the more effective control of the O₃ formation, which providing important
42 scientific support for the management department for better formulation and implementation of measures
43 on photochemical pollution.

44 Indeed, more and more policies on VOCs were/are being implemented and formulated in the PRD region
45 and/or the whole country. A series of policies regarding the control of vehicular emissions have been
46 conducted in the PRD region, which can be mainly divided into two categories: 1) Improve the
47 environment standards of the main air pollutants, *e.g.*, the National Ambient Air Quality Standard of GB
48 3095-2012; 2) Improve the quality of the fuel used in vehicles, *e.g.* the fifth phase of the vehicle emission
49 standards (GB 18176-2016, GB 14622-2016, GB 19755-2016, and HJ 689-2014). It should be noted that
50 the fifth phase of the vehicle emission standards have limited the emissions of total VOCs from vehicles
51 (IGES, 2014) compared with those of the fourth phase. On 26 December 2017, the Monitoring Plan on
52 the Ambient Volatile Organic Compounds (VOCs) in Key Areas in 2018 was issued by the Ministry of
53 Environmental Protection, which will help to better supervise and provide more observed data for
54 exploring the effective pathways to alleviate VOCs and photochemical O₃ pollution. In addition, “new
55 energy automobiles” are promoted widely in urban cities of the PRD region, such as Guangzhou and
56 Shenzhen, and the eight civil conduct codes of “Breath and Struggle together” were released to raise the
57 public’s concern about how to improve the air quality. However, the policies on controlling biomass
58 burning are relatively limited when compared to those for vehicular emissions. For biomass burning,
59 straw return and collected integrated agricultural machinery have been encouraged and widely promoted,
60 and the outdoor burning of straw was forbidden according to the Law of the Prevention and Control of



61 Atmospheric Pollution. The emission standards for biomass burning are included in the latest version of
62 “Air pollution emission standard for boilers” (GB 13271-2014), where emission standards of coal-fired
63 boilers were applied to biomass briquettes. Furthermore, the emissions from biomass forming fuel boilers
64 and the biomass-molded fuel used in Guangdong should meet DB44/765-2017 and DB44/T 1052-2012,
65 respectively.

66 Nevertheless, it is expected that these measures could help alleviate the photochemical pollution and
67 improve air quality and visibility, but most of them only control the total mass of VOCs. Therefore,
68 evaluation on the benefits of these measures on VOCs and photochemical pollution is still needed. Overall,
69 the findings of this study provide quantitative information on devising appropriate measures on the VOCs,
70 NO_x, and O₃ pollution at the receptor site of PRD, which could be extended to other regions in China.

71

72 **Competing interests**

73 The authors declare that they have no conflict of interest.

74

75 **Author Contributions**

76 In this study, the analysis methods were developed and the whole structure for the manuscript was
77 designed by Dr. Zhenhao Ling, Dr. Zhe Wang and Prof. Jun Zhao. Ms. Zhuoran He conducted the data
78 process and wrote the original copy of the manuscript. Prof. Xuemei Wang and Prof. Min Shao provided
79 the data and revised the manuscript. Furthermore, the simulation of PBM-MCM model was conducted by
80 Dr. Zhenhao Ling and Prof. Hai Guo. Finally, the manuscript was finalized by Dr. Zhenhao Ling and
81 Dr. Zhe Wang.



82 Acknowledgements

83 This study was supported by the National Key Research and Development Program of China
84 (2017YFC0210106, 2016YFC0203305), the State Key Program of National Natural Science Foundation
85 of China (No. 91644215), the National Natural Science Foundation of China (No. 41775114 and
86 41505103) and Hong Kong Research Grants Council (25221215, 15265516).

87 References

- 88 Atkinson, R., Baulch, D. L., Cox, R. A., Crowley, J. N., Hampson, R. F., Hynes, R. G., Jenkin, M. E., Rossi, M. J., Troe,
89 J., and IUPAC Subcommittee: Evaluated kinetic and photochemical data for atmospheric chemistry: Volume II –
90 gas phase reactions of organic species, *Atmos. Chem. Phys.*, 6, 3625-4055, [https://doi.org/10.5194/acp-6-3625-](https://doi.org/10.5194/acp-6-3625-2006)
91 2006, 2006.
- 92 ATSDR, Agency for Toxic Substances and Diseases Registry, <http://www.atsdr.cdc.gov/toxfaqs/index.asp>, 2007.
- 93 Blake, D. R., Smith, Jr. T., Chen, T. Y., Whipple, W., and Rowland, F. S: Effects of biomass burning on summertime
94 nonmethane hydrocarbon concentrations in the Canadian wetlands. *J. Geophys. Res.-Atmos.*, 99, 1699-1719.
95 <https://doi.org/10.1029/93JD02598>, 1994.
- 96 Cai, C. J., Geng, F. H., Tie, X. X., Yu, Q., and An, J. L.: Characteristics and source apportionment of VOC measured in
97 Shanghai, China, *Atmos. Environ.*, 44, 5005-5014, <https://doi.org/10.1016/j.atmosenv.2010.07.059>, 2010.
- 98 Cardelino, C. A., and Chameides, W. L: An observation-based model for analyzing ozone precursor relationships in the
99 urban atmosphere, *J. Air Waste Manage.*, 45, 161-80. <https://doi.org/10.1080/10473289.1995.10467356>, 1995.
- 00 Carter, W. L., and Atkinson, R.: Computer modeling study of incremental hydrocarbon reactivity, *Environ. Sci. Technol.*,
01 23, 864-880, <https://doi.org/10.1021/es00065a017>, 1989.
- 02 Chan, L. Y., Chu, K. W., Zou, S. C., Chan, C. Y., Wang, X. M., Barletta, B., Blake, D. R., Guo, H., and Tsai, W. Y.:
03 Characteristics of nonmethane hydrocarbons (NMHCs) in industrial, industrial-urban, and industrial-suburban



- 04 atmospheres of the Pearl River Delta (PRD) region of south China, *J. Geophys. Res.-Atmos.*, 111, 9,
05 <https://doi.org/10.1029/2005JD006481>, 2006.
- 06 Chang, C., Wang, J. L., Liu, S., Shao, M. Z., Zhang, Y., Zhu, T. J., Shiu, C., and Lai, C.: Photochemically consumed
07 hydrocarbons and their relationship with ozone formation in two megacities of China, *Agu Fall Meeting, AGU Fall*
08 *Meeting Abstracts*, 2010.
- 09 Cheng, H. R., Guo, H., Wang, X. M., Saunders, S. M., Lam, S. H. M., Jiang, F., Wang, T. J., Ding, A. J., Lee, S. C., and
10 Ho, K. F.: On the relationship between ozone and its precursors in the Pearl River Delta: application of an
11 observation-based model (OBM), *Environ. Sci. Pollut. R.*, 17, 547-560, [https://doi.org/10.1007/s11356-009-0247-](https://doi.org/10.1007/s11356-009-0247-9)
12 9, 2010.
- 13 de Gouw, J. A., Middlebrook, A. M., Warneke, C., Goldan, P. D., Kuster, W. C., Roberts, J. M., Fehsenfeld, F. C.,
14 Worsnop, D. R., Canagaratna, M. R., Pszenny, A. A. P., Keene, W. C., Marchewka, M., Bertman, S., and Bates, T.
15 S.: Budget of organic carbon in a polluted atmosphere: Results from the New England Air Quality Study in 2002,
16 *J. Geophys. Res.-Atmos.*, 110, D16305, <https://doi.org/10.1029/2004JD005623>, 2005.
- 17 Duan, J. C., Tan, J. H., Yang, L., Wu, S., and Hao, J. M.: Concentration, sources and ozone formation potential of volatile
18 organic compounds (VOCs) during ozone episode in Beijing, *Atmos. Res.*, 88, 25-35,
19 <https://doi.org/10.1016/j.atmosres.2007.09.004>, 2008.
- 20 Fuentes, J. D., Wang, D., Neumann, H. H., Gillespie, T. J., Hartog, G. D., and Dann, T. F.: Ambient biogenic
21 hydrocarbons and isoprene emissions from a mixed deciduous forest, *J. Atmos. Chem.*, 25, 67-95,
22 <https://doi.org/10.1007/BF00053286>, 1996.
- 23 Geng, F., Cai, C., Tie, X., Yu, Q., An, J., Peng, L., and Xu, J.: Analysis of VOC emissions using PCA/APCS receptor
24 model at city of Shanghai, China, *J. Atmos. Chem.*, 62, 229-247, <https://doi.org/10.1007/s10874-010-9150-5>, 2009.
- 25 Guo, H., Cheng, H. R., Ling, Z. H., Louie, P. K. K., and Ayoko, G. A.: Which emission sources are responsible for the
26 volatile organic compounds in the atmosphere of Pearl River Delta?, *J. Hazard. Mater.*, 188, 116-124,
27 <https://doi.org/10.1016/j.jhazmat.2011.01.081>, 2011a.



- 28 Guo, H., Ling, Z. H., Cheng, H. R., Simpson, I. J., Lyu, X. P., Wang, X. M., Shao, M., Lu, H. X., Ayoko, G., Zhang, Y.
29 L., Saunders, S. M., Lam, S. H. M., Wang, J. L., and Blake, D. R.: Tropospheric volatile organic compounds in
30 China, *Sci. Total Environ.*, 574, 1021-1043, <https://doi.org/10.1016/j.scitotenv.2016.09.116>, 2017.
- 31 Guo, H., Zou, S. C., Tsai, W. Y., Chan, L. Y., and Blake, D. R.: Emission characteristics of non-methane hydrocarbons
32 from private cars and taxis at different driving speeds in Hong Kong, *Atmos. Environ.*, 45, 2711-2721,
33 <https://doi.org/10.1016/j.atmosenv.2011.02.053>, 2011b.
- 34 He, J., Chen, H. X., Liu, X. X., Hu, J. H., Li, Q. L., and He, F. Q.: The analysis of various volatile solvents used in
35 different industries in Zhongshan (in Chinese), *South China Journal of Preventive Medicine*, 28(6), 26-27.
36 <https://doi.org/10.3969/j.issn.1671-5039.2002.06.009>, 2002.
- 37 Ho, K. F., Lee, S. C., Ho, W. K., Blake, D. R., Cheng, Y., Li, Y. S., Ho, S. S. H., Fung, K., Louie, P. K. K., and Park,
38 D.: Vehicular emission of volatile organic compounds (VOCs) from a tunnel study in Hong Kong, *Atmos. Chem.*
39 *Phys.*, 9, 7491-7504, <https://doi.org/10.5194/acp-9-7491-2009>, 2009.
- 40 Holzinger, R., Warneke, C., Hansel, A., Jordan, A. and Lindinger, W.: Biomass burning as a source of formaldehyde,
41 acetaldehyde, methanol, acetone, acetonitrile, and hydrogen cyanide, *Geophys. Res. Lett.*, 26, 1161-1164,
42 <https://doi.org/10.1029/1999GL900156>, 1999.
- 43 Huang, R. J., Zhang, Y., Bozzetti, C., Ho, K. F., Cao, J. J., Han, Y., Daellenbach, K. R., Slowik, J. G., Platt, S. M.,
44 Canonaco, F., et al.: High secondary aerosol contribution to particulate pollution during haze events in China,
45 *Nature*, 514, 218-222, <https://doi.org/10.1038/nature13774>, 2014.
- 46 Jenkin, M. E. and Clemitshaw, K. C.: Ozone and other secondary photochemical pollutants: chemical processes
47 governing their formation in the planetary boundary layer, *Atmos. Environ.*, 34, 2499-2527,
48 [https://doi.org/10.1016/S1352-2310\(99\)00478-1](https://doi.org/10.1016/S1352-2310(99)00478-1), 2000.
- 49 Jimenez, J. L., Canagaratna, M. R., Donahue, N. M., Prevot, A. S. H., Zhang, Q., Kroll, J. H., DeCarlo, P. F., Allan, J.
50 D., Coe, H., Ng, N. L., et al.: Evolution of organic aerosols in the atmosphere, *Science*, 326(5959), 1525-1529.
51 <https://doi.org/10.1126/science.1180353>, 2009.



- 52 Lam, S. H. M., Saunders, S. M., Guo, H., Ling, Z. H., Jiang, F., Wang, X. M., and Wang, T. J.: Modelling VOC source
53 impacts on high ozone episode days observed at a mountain summit in Hong Kong under the influence of mountain-
54 valley breezes, *Atmos. Environ.*, 81, 166-176, <https://doi.org/10.1016/j.atmosenv.2013.08.060>, 2013.
- 55 Lau, A. K. H., Yuan, Z., Yu, J. Z., and Louie, P. K.: Source apportionment of ambient volatile organic compounds in
56 Hong Kong, *Sci. Total Environ.*, 408, 4138-4149, <https://doi.org/10.1016/j.scitotenv.2010.05.025>, 2010.
- 57 Li, J. F., Lu, K. D., Lv, W., Li, J., Zhong, L. J., Ou, Y. B., Chen, D. H., Huang, X., and Zhang, Y. H.: Fast increasing of
58 surface ozone concentrations in Pearl River Delta characterized by a regional air quality monitoring network during
59 2006-2011, *J. Environ. Sci.*, 26, 23-36, [https://doi.org/10.1016/S1001-0742\(13\)60377-0](https://doi.org/10.1016/S1001-0742(13)60377-0), 2014.
- 60 Li, L. Y., Xie, S. D., Zeng, L. M., Wu, R. R., and Li, J.: Characteristics of volatile organic compounds and their role in
61 ground-level ozone formation in the Beijing-Tianjin-Hebei region, China, *Atmos. Environ.*, 113, 247-254,
62 <https://doi.org/10.1016/j.atmosenv.2015.05.021>, 2015.
- 63 Ling, Z. H., and Guo, H.: Contribution of VOC sources to photochemical ozone formation and its control policy
64 implication in Hong Kong, *Environ. Sci. Pollut. Res.*, 38, 180-191, <https://doi.org/10.1016/j.envsci.2013.12.004>,
65 2014.
- 66 Ling, Z. H., Guo, H., Cheng, H. R., and Yu, Y. F.: Sources of ambient volatile organic compounds and their contributions
67 to photochemical ozone formation at a site in the Pearl River Delta, southern China, *Environ. Pollut.*, 159, 2310-
68 2319, <https://doi.org/10.1016/j.envpol.2011.05.001>, 2011.
- 69 Ling, Z. H., Zhao, J., Fan, S. J., and Wang, X. M.: Sources of formaldehyde and their contributions to photochemical O₃
70 formation at an urban site in the Pearl River Delta, southern China, *Chemosphere*, 168, 1293-1301,
71 <https://doi.org/10.1016/j.chemosphere.2016.11.140>, 2017.
- 72 Liu, Y., Shao, M., Kuster, W. C., Goldan, P. D., Li, X. H., Lu, S. H., and de Gouw, J. A.: Source identification of reactive
73 hydrocarbons and oxygenated VOCs in the summertime in Beijing, *Environ. Sci. Technol.*, 43, 75-81,
74 <https://doi.org/10.1021/es801716n>, 2009.



- 75 Liu, Y., Shao, M., Lu, S. H., Chang, C. C., Wang, J. L., and Fu, L. L.: Source apportionment of ambient volatile organic
76 compounds in the Pearl River Delta, China: Part II, Atmos. Environ., 42, 6261-6274,
77 <https://doi.org/10.1016/j.atmosenv.2008.02.027>, 2008.
- 78 Lyu, X., Guo, H., Simpson, I. J., Meinardi, S., Louie, P. K. K., Ling, Z., Wang, Y., Liu, M., Luk, C. W. Y., Wang, N.,
79 and Blake, D. R.: Effectiveness of replacing catalytic converters in LPG-fueled vehicles in Hong Kong, Atmos.
80 Chem. Phys., 16, 6609-6626, <https://doi.org/10.5194/acp-16-6609-2016>, 2016.
- 81 Nelson, P. F., and Quigley, S. M.: The hydrocarbon composition of exhaust emitted from gasoline fueled vehicles, Atmos.
82 Environ., 18, 79-87, [https://doi.org/10.1016/0004-6981\(84\)90230-0](https://doi.org/10.1016/0004-6981(84)90230-0), 1984.
- 83 Ou, J. M., Feng, X. Q., Liu, Y. C., Gao, Z. Z., Yang, Y., Zhou, Z., Wang, X. M., and Zheng J. Y.: Source characteristics
84 of VOCs emissions from vehicular exhaust in the Pearl River Delta region, Acta Scientiae Circumstantiae, 34, 826-
85 834, <https://doi.org/10.13671/j.hjkxxb.2014.0614>, 2014.
- 86 Ou, J. M., Guo, H., Zheng, J. Y., Cheung, K. L., Louie, P. K. K., Ling, Z. H., and Wang, D. W.: Concentrations and
87 sources of non-methane hydrocarbons (VOCs) from 2005 to 2013 in Hong Kong: a multi-year real-time analysis,
88 Atmos. Environ., 103, 196-206, <https://doi.org/10.1016/j.atmosenv.2014.12.048>, 2015a.
- 89 Ou, J. M., Zheng, J. Y., Li, R. R., Huang, X. B., Zhong, Z. M., Zhong, L. J., and Lin, H.: Speciated OVOC and VOC
90 emission inventories and their implications for reactivity-based ozone control strategy in the Pearl River Delta
91 region, China, Sci. Total Environ., 530-531, 393-402, <https://doi.org/10.1016/j.scitotenv.2015.05.062>, 2015b.
- 92 Paatero, P.: Least squares formulation of robust non-negative factor analysis, Chemometr. Intell. Lab., 37, 23-35,
93 [https://doi.org/10.1016/S0169-7439\(96\)00044-5](https://doi.org/10.1016/S0169-7439(96)00044-5), 1997.
- 94 Paatero, P.: User's guide for positive matrix factorization programs PMF2 and PMF3, part 1: tutorial, Prepared by
95 University of Heisinki, Finland, February, 2000a.
- 96 Paatero, P.: User's guide for positive matrix factorization programs PMF2 and PMF3, part 2: Reference, Prepared by
97 University of Heisinki, Finland, February, 2000b.
- 98 Paatero, P., and Tapper, U.: Positive matrix factorization: a non-negative factor model with optimal utilization of error
99 estimates of data values, Environment, 5, 111-126, <https://doi.org/10.1002/env.3170050203>, 1994.



- 00 Rudolph, J.: The tropospheric distribution and budget of ethane, *J. Geophys. Res.*, 100, 11369-11381,
01 <https://doi.org/10.1029/95JD00693>, 1995.
- 02 Sanadze, G. A.: Biogenic Isoprene (A Review), *Russian Journal of Plant Physiology*, 51, 729-741, 2004.
- 03 Saunders, S. M., Jenkin, M. E., Derwent, R. G., and Pilling, M. J.: Protocol for the development of the Master Chemical
04 Mechanism, MCM v3 (Part A): tropospheric degradation of non-aromatic volatile organic compounds, *Atmos.*
05 *Chem. Phys.*, 3, 161-180, <https://doi.org/10.5194/acp-3-161-2003>, 2003.
- 06 Seinfeld, J. H., and Pandis, S. N.: *Atmospheric Chemistry and Physics: from air pollution to climate change*, John Wiley,
07 New York, NY, 2006.
- 08 Shao, M., Lu, S. H., Liu, Y., Xie, X., Chang, C. C., Huang, S., and Chen, Z. M.: Volatile organic compounds measured
09 in summer in Beijing and their role in ground-level ozone formation, *J. Geophys. Res.*, 114, D00G06,
10 <https://doi.org/10.1029/2008JD010863>, 2009.
- 11 Shiu, C. J., Liu, S. C., Chang, C. C., Chen, J. P., Chou, C. K., Lin, C. Y., and Young, C. Y.: Photochemical production
12 of ozone and control strategy for southern Taiwan, *Atmos. Environ.*, 41, 9324-9340,
13 <https://doi.org/10.1016/j.atmosenv.2007.09.014>, 2007.
- 14 Song, C. L., Zhang, W. M., Pei, Y. Q., Fan, G. L. and Xu, G. P.: Comparative effects of MTBE and ethanol additions
15 into gasoline on exhaust emissions, *Atmos. Environ.*, 40, 1957-1970,
16 <https://doi.org/10.1016/j.atmosenv.2005.11.028>, 2006.
- 17 Song, Y., Shao, M., Liu, Y., Lu, S., Kuster, W., Goldan, P., and Xie, S.: Source apportionment of ambient volatile organic
18 compounds in Beijing, *Environ. Sci. Technol.*, 41, 4348-4353, <https://doi.org/10.1021/es0625982>, 2007.
- 19 Tang, J. H., Chan, L. Y., Chang, C. C., Liu, S., and Li, Y. S.: Characteristics and sources of nonmethane hydrocarbons
20 in background atmospheres of eastern, southwestern, and southern China, *J. Geophys. Res.-Atmos.*, 114, D3,
21 <https://doi.org/10.1029/2008JD010333>, 2009.
- 22 Wadden, R. A., Uno, I., and Wakamatsu, S.: Source discrimination of short-term hydrocarbon samples measured aloft,
23 *Environ. Sci. Technol.*, 20, 473-483, <https://doi.org/10.1021/es00147a006>, 1986.



- 24 Wang, J. L., Wang, C. H., Lai, C. H., Chang, C. C., Liu, Y., Zhang, Y., Liu, S., and Shao, M.: Characterization of ozone
25 precursors in the Pearl River Delta by time series observation of non-methane hydrocarbons, *Atmos. Environ.*, 42,
26 6233-6246, <https://doi.org/10.1016/j.atmosenv.2008.01.050>, 2008.
- 27 Wang, Y., Wang, H., Guo, H., Lyu, X., Cheng, H., Ling, Z., Louie, P. K. K., Simpson, I. J., Meinardi, S., and Blake, D.
28 R.: Long-term O₃-precursor relationships in Hong Kong: field observation and model simulation, *Atmos. Chem.*
29 *Phys.*, 17, 10919-10935, <https://doi.org/10.5194/acp-17-10919-2017>, 2017.
- 30 Yang, Y., Shao, M., Keßel, S., Li, Y., Lu, K., Lu, S., Williams, J., Zhang, Y., Zeng, L., Nölscher, A. C., Wu, Y., Wang,
31 X., and Zheng, J.: How the OH reactivity affects the ozone production efficiency: case studies in Beijing and Heshan,
32 China, *Atmos. Chem. Phys.*, 17, 7127-7142, <https://doi.org/10.5194/acp-17-7127-2017>, 2017.
- 33 Yuan, B., Chen, W. T., Shao, M., Wang, M., Lu, S. H., Wang, B., Liu, Y., Chang, C. C., Wang, B. G.: Measurements of
34 ambient hydrocarbons and carbonyls in the Pearl River Delta (PRD), China, *Atmos. Res.*, 116, 93-104,
35 <https://doi.org/10.1016/j.atmosres.2012.03.006>, 2012a.
- 36 Yuan, B., Liu, Y., Shao, M., Lu, S., and Streets, D. G.: Biomass Burning Contributions to Ambient VOCs Species at a
37 Receptor Site in the Pearl River Delta (PRD), China. *Environ. Sci. Technol.*, 44, 4577,
38 <https://doi.org/10.1021/es1003389>, 2010.
- 39 Yuan, B., Shao, M., de Gouw, J., Parrish, D. D., Lu, S. H., Wang, M., Zeng, L. M., Zhang, Q., Song, Y., Zhang, J. B.,
40 and Hu, M.: Volatile organic compounds (VOCs) in urban air: How chemistry affects the interpretation of positive
41 matrix factorization (PMF) analysis, *J. Geophys. Res.*, 117, D24302, <https://doi.org/10.1029/2012JD018236>, 2012b.
- 42 Yuan, Z.B., Lau, A.K.H., Shao, M., Louie, P.K.K., Liu, S.C., Zhu, T.: Source analysis of volatile organic compounds by
43 positive matrix factorization in urban and rural environments in Beijing. *J. Geophys. Res.*, 114, D00G15,
44 [doi:10.1029/2008JD011190](https://doi.org/10.1029/2008JD011190), 2009.
- 45 Zhang, Q., Yuan, B., Shao, M., Wang, X., Lu, S., Lu, K., Wang, M., Chen, L., Chang, C.-C., and Liu, S. C.: Variations
46 of ground-level O₃ and its precursors in Beijing in summertime between 2005 and 2011, *Atmos. Chem. Phys.*, 14,
47 6089-6101, <https://doi.org/10.5194/acp-14-6089-2014>, 2014.



- 48 Zhang, Y. H., Hu, M., Zhong, L. J., Wiedensohler, A., Liu, S. C., Andreae, M. O., Wang, W., and Fan, S. J.: Regional
49 integrated experiments on air quality over Pearl River Delta 2004 (PRIDE-PRD2004): Overview, Atmos. Environ.,
50 42, 6157-6173, <https://doi.org/10.1016/j.atmosenv.2008.03.025>, 2008a.
- 51 Zhang, Y. H., Su, H., Zhong, L. J., Cheng, Y. F., Zeng, L. M., Wang, X. S., Xiang, Y. R., Wang, J. L., Gao, D. F., Shao,
52 M., Fan, S. J., Liu, S. C.: Regional ozone pollution and observation-based approach for analyzing ozone-precursor
53 relationship during the PRIDE-PRD2004 campaign, Atmos. Environ., 42, 6203-6218,
54 <https://doi.org/10.1016/j.atmosenv.2008.05.002>, 2008.
- 55 Zhang, Y. L., Wang, X. M., Barletta, B., Simpson, I. J., Blake, D. R., Fu, X. X., Zhang, Z., He, Q. F., Liu, T. Y., Zhao,
56 X. Y., and Ding, X.: Source attributions of hazardous aromatic hydrocarbons in urban, suburban and rural areas in
57 the Pearl River Delta (PRD) region, J. Hazard. Mater., 250-251, 403-411,
58 <https://doi.org/10.1016/j.jhazmat.2013.02.023>, 2013.
- 59 Zheng, J. Y., Yu, Y. F., Mo, Z. W., Zhang, Z., Wang, X. M., Yin, S. S., Peng, K., Yang, Y., Feng, X. Q., and Cai, H. H.:
60 Industrial sector-based volatile organic compound (VOC) source profiles measured in manufacturing facilities in
61 the Pearl River Delta, China, Sci. Total Environ., 456-457, 127-136, <https://doi.org/10.1016/j.scitotenv.2013.03.055>,
62 2013.
- 63 Zheng, J. Y., Zhang, L. J., Che, W. W., Zheng, Z. Y., and Yin, S. S.: A highly resolved temporal and spatial air pollutant
64 emission inventory for the Pearl River Delta, China and its uncertainty assessment, Atmos. Environ., 43, 5112-5122,
65 <https://doi.org/10.1016/j.atmosenv.2009.04.060>, 2009.
- 66 Zheng, J. Y., Zhong, L. J., Wang, T., Louie, P. K. K., and Li, Z. C.: Ground-level ozone in the Pearl River Delta region:
67 analysis of data from a recently established regional air quality monitoring network, Atmos. Environ., 44, 814-823,
68 <https://doi.org/10.1016/j.atmosenv.2009.11.032>, 2010.
- 69 Zhou, Y., Zhong, L. J., Yue, D. L., Zeng, L. M., and Zhang, T.: Potential Ozone Formation and Emission Sources of
70 Atmospheric VOCs in Heshan during Typical Pollution Episode (In Chinese), Environmental Monitoring and
71 Forewarning, 6, 1-16, <https://doi.org/10.3969/j.issn.1674-6732.2014.04.001>, 2014.



- .72 Zhou, Y., Yue, D. L., Zhong, L. J., and Zeng, L. M.: Properties of atmospheric PAN pollution in Heshan during summer
.73 time. *The Administration and Technique of Environmental Monitoring*, 4, 24-27, 2013.
- .74 Zhu, Y. H., Yang, L. X., Chen, J. M., Wang, X. F., Xue, L. K., Sui, X., Wen, L., Xu, C. H., Yao, L., Zhang, J. M., Shao,
.75 M., Lu, S. H., and Wang, W. X.: Characteristics of ambient volatile organic compounds and the influence of biomass
.76 burning at a rural site in Northern China during summer 2013, *Atmos. Environ.*, 124, 156-165,
.77 <https://doi.org/10.1016/j.atmosenv.2015.08.097>, 2016.
- .78 Zou, Y., Deng, X. J., Zhu, D., Gong, D. C., Wang, H., Li, F., Tan, H. B., Deng, T., Mai, B. R., Liu, X. T., and Wang, B.
.79 G.: Characteristics of 1 year of observational data of VOCs, NO_x and O₃ at a suburban site in Guangzhou, China,
.80 *Atmos. Chem. Phys.*, 15, 6625-6636, <https://doi.org/10.5194/acp-15-6625-2015>, 2015.